arXiv:1404.5394v1 [nlin.CD] 22 Apr 2014

Ghost-vibrational resonance

S Rajamani, S Rajasekar

School of Physics, Bharathidasan University, Tiruchirappalli 620 024, India

MAF Sanjuán

Nonlinear Dynamics, Chaos and Complex Systems Group, Departamento de Física, Universidad Rey Juan Carlos, Tulipán s/n, 28933 Móstoles, Madrid, Spain

Abstract

Ghost-stochastic resonance is a noise-induced resonance at a fundamental frequency missing in the input signal. We investigate the effect of a high-frequency, instead of a noise, in a single Duffing oscillator driven by a multi-frequency signal $F(t) = \sum_{i=1}^{n} f_i \cos(\omega_i + \Delta\omega_0)t$, $\omega_i = (k + i - 1)\omega_0$, where k is an integer greater than or equal to two. We show the occurrence of a high-frequency induced resonance at the missing fundamental frequency ω_0. For the case of the two-frequency input signal, we obtain an analytical expression for the amplitude of the periodic component with the missing frequency. We present the influence of the number of forces n, the parameter k, the frequency ω_0 and the frequency shift $\Delta\omega_0$ on the response amplitude at the frequency ω_0. We also investigate the signal propagation in a network of unidirectionally coupled Duffing oscillators. Finally, we show the enhanced signal propagation in the coupled oscillators in absence of a high-frequency periodic force.

Keywords: Ghost resonance, multi-frequency signal, Duffing oscillator.

1. Introduction

Response of nonlinear systems to a harmonic force with a single frequency has been investigated in detail. A non-monotonic variation of the amplitude

Email addresses: rajeebard@gmail.com (S Rajamani), rajasekar@cnld.bdu.ac.in (S Rajasekar), miguel.sanjuan@urjc.es (MAF Sanjuán)

of the response occurs [1, 2], in a typical nonlinear system when the frequency of the driving force is varied. In particular, the oscillation amplitude of the system output increases with the increase in the frequency of the external force, it reaches a maximum at a particular frequency and then it decreases with further increase in the frequency. This resonance phenomenon is widespread and has been utilized in several devices. In bistable and multistable systems when the amplitude of the external periodic force is below a threshold (that is, there is no switching motion between the coexisting stable states), then a transition between the coexisting states can be induced by a weak noise. At an appropriate optimum noise intensity, almost a periodic switching between coexisting states occurs resulting in a maximum system response. This noise-induced resonance phenomenon is termed as *stochastic resonance* [3, 4]. Resonance can be realized when the noise term is replaced by a high-frequency periodic force and is called *vibrational resonance* [5, 6]. Furthermore, it is possible to generate a chaotic signal that mimics the probability distribution of the Gaussian white noise. Such a signal can also give rise to a resonant effect analogous to the noise-induced resonance and is called *chaotic resonance* [7]. In all the above resonance phenomena, in absence of a resonance inducing source, the system is driven by a weak harmonic force with a single frequency. There are signals with multiple frequencies. Examples include human speech, musical tones and square-waves. Design of an approximate multi-frequency signal is very important in minimizing the nonlinear distortion in the multi-frequency system identification methods [8, 9].

Chialvo et al. [10, 11] investigated the response of a threshold device to an input signal containing several frequencies in the presence of noise. When the frequencies of the driving force are of a higher-order of a certain fundamental frequency, then the system is found to show a maximum response at the missing fundamental frequency at an optimum noise intensity. This fundamental frequency, which is absent in the input signal, detected by the device is called ghost-frequency and the underlying resonance phenomenon is termed as *ghost-stochastic resonance* [10, 11]. When the input signal is set into an anharmonic by introducing a same frequency shift to all the harmonic terms, the system is found to show a resonance at a certain shifted frequency. This ghost resonance phenomenon can be used to explain the missing fundamental illusion in which a third lower pitched tone is often heard when two tones occur together [11].

The occurrence of a ghost resonance induced by noise has been analysed mostly in excitable systems. For example, it was found in the sudden

dropouts exhibited by a semiconductor laser [12], two laser systems coupled bidirectionally [13], vertical-cavity surface emitting lasers [14], monostable Schmitt trigger electronic circuit [15], an excitable Chua's circuit [16], a chaotic Chua's circuit [17] and a system of n-coupled neurons [18]. Subharmonic resonance behaviour in a nonlinear system with a multi-frequency force containing the fundamental frequency in the absence of a high-frequency input signal is studied in [19].

Because nonlinear systems with double-well and multi-well potentials are wide-spread it is foremost important to investigate the response of these systems to the multi-frequency force and analyse the occurrence of ghost resonance in them and also with sources other than external noise. Motivated by the above considerations, in the present work, we explore the possibility of a ghost resonance induced by a high-frequency deterministic force rather than a noise. We consider the Duffing oscillator driven by multi-frequency force $F(t)$ and a high-frequency force $g\cos\Omega t$. The multi-frequency force $F(t)$ is given by

$$F(t) = \sum_{i=1}^{n} f_i \cos(\omega_i + \Delta\omega_0)t, \quad \omega_i = (k+i-1)\omega_0 \tag{1}$$

with $k \geq 2$ and $\Omega \gg \omega_n (= (k+n-1)\omega_0)$. We begin our analysis with $n = 2$, $k = 2$ and $\Delta\omega_0 = 0$. We show the occurrence of a resonance at the fundamental frequency ω_0 missing in the input signal $F(t)$. The value of g at which the resonance at the frequency ω_0 occurs, increases monotonically while the value of the response amplitude $Q(\omega_0)$ at resonance decreases with ω_0. Interestingly, the case of $n = 2$ by applying a theoretical method, we are able to obtain an approximate analytical expression for the response amplitudes $Q(\omega_i)$, $i = 0, 1, 2$. Theoretical results are in good agreement with the numerical predictions. We study the influence of the number of periodic forces n, the parameters k and g and the frequency shift $\Delta\omega_0$ on $Q(\omega_0)$. For values of $k > 2$ or $\Delta\omega_0 \neq 0$, the response amplitude $Q(\omega_0)$ becomes 0 when the oscillation center of the orbit is at the origin and this happens for g values above a certain critical value.

Next, we consider a network of unidirectionally coupled N-Duffing oscillators with the multi-frequency force and the high-frequency force applied to the first oscillator only. The first system is uncoupled. The coupling term is chosen to be linear. We denote $Q_i(\omega_0)$ as the response amplitude of the ith oscillator at the frequency ω_0. For a coupling strength above a critical

value, an undamped signal propagation, that is, $Q_N(\omega_0) > Q_1(\omega_0)$ occurs at the missing fundamental frequency, even in the absence of the high-frequency periodic force. Interestingly, in the undamped signal propagation case, the response amplitude increases with the unit number i and then becoming a constant. The saturation value of Q is found to be independent of the parameters k, n and $\Delta\omega_0$ in $F(t)$. Finally, we consider a network of unidirectionally coupled oscillators, where all the oscillators are driven by the external forces.

2. Resonance in a single Duffing oscillator

We consider the equation of motion of the Duffing oscillator driven by n harmonic forces $F(t)$ given by Eq. (1) and the high-frequency periodic force $g\cos\Omega t$ as

$$\ddot{x} + d\dot{x} + \alpha x + \beta x^3 = F(t) + g\cos\Omega t. \tag{2}$$

Throughout our study we fix the values of the parameters as $d = 0.5$, $\alpha = -2$, $\omega_0 = 0.5$, $\beta = 1$, $\Omega = 30\omega_0$ and treat g as the control parameter. The potential associated to the system in the absence of damping and external force is of a double-well form, since $\alpha < 0$ and $\beta > 0$.

2.1. Numerical analysis

From the numerical solution of Eq. (2), we compute the sine and cosine components $Q_{\rm s}(\omega)$ and $Q_{\rm c}(\omega)$ respectively of the solution at various frequencies in the interval $\omega \in [0, 20]$ using the equations

$$Q_{\rm s}(\omega) = \frac{2}{NT}\int_0^{NT} x(t)\sin\omega t\, dt, \tag{3a}$$

$$Q_{\rm c}(\omega) = \frac{2}{NT}\int_0^{NT} x(t)\cos\omega t\, dt, \tag{3b}$$

where $T = 2\pi/\omega$ and N is say 500. Then $Q(\omega) = \sqrt{Q_{\rm s}^2 + Q_{\rm c}^2}/f$ with $f = (1/n)\sum_{i=1}^{n} f_i$.

First, we consider the system (2) with $n = 2$, $k = 2$ and $\Delta\omega_0 = 0$, that is $F(t) = f_1\cos\omega_1 t + f_2\cos\omega_2 t$ where $\omega_1 = 2\omega_0$, $\omega_2 = 3\omega_0$ and $\omega_0 = 0.5$. We compute $Q(\omega_0)$, $Q(2\omega_0)$ and $Q(3\omega_0)$ for (i) $f_1 = f$, $f_2 = 0$, (ii) $f_1 = 0$, $f_2 = f$ and (iii) $f_1 = f_2 = f$ with $f = 0.1$. Figure 1 shows the variation of numerically computed $Q(2\omega_0)$ with the parameter g for the cases (i) and

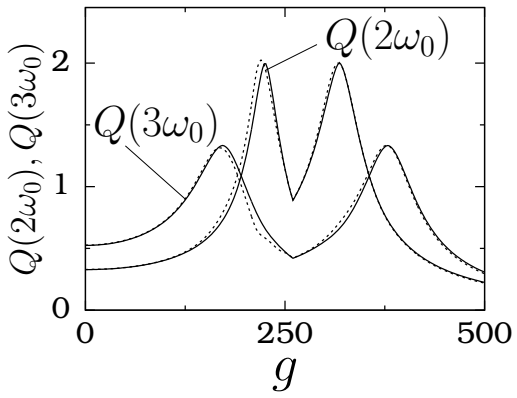

Figure 1: $Q(2\omega_0)$ and $Q(3\omega_0)$ versus g of the system (2) with $F(t) = f_1 \cos 2\omega_0 t + f_2 \cos 3\omega_0 t$ for the cases (i) $f_1 = 0.1$, $f_2 = 0$ ($Q(2\omega_0) \neq 0$ (continuous curve), $Q(3\omega_0) = 0$), (ii) $f_1 = 0$, $f_2 = 0.1$ ($Q(2\omega_0) = 0$, $Q(3\omega_0) \neq 0$ (continuous curve)) and (iii) $f_1 = f_2 = 0.1$ (both $Q(2\omega_0)$ and $Q(3\omega_0)$ are nonzero and are represented by dashed curves).

(iii) (represented by continuous and dashed curves respectively) and $Q(3\omega_0)$ for the cases (ii) and (iii) (continuous and dashed curves respectively). For $f_2 = 0$, $Q(3\omega_0) = 0$ while for $f_1 = 0$, $Q(2\omega_0) = 0$. In both cases $Q(\omega_0) = 0$. When $f_1 \neq 0$ and $f_2 \neq 0$ both $Q(2\omega_0)$ and $Q(3\omega_0)$ are present in the solution of the system (2). Q at $\omega = 2\omega_0$ and $3\omega_0$ exhibits resonance. For a wide range of g, $Q(2\omega_0)$ of the cases (i) and (iii) are almost the same. This result is observed for $Q(3\omega_0)$ except for the values of g near the first resonance of $Q(2\omega_0)$. We can say that there is no significant effect of the presence of the periodic force $f_1 \cos 2\omega_0 t$ on $Q(3\omega_0)$ and $f_2 \cos 3\omega_0 t$ on $Q(2\omega_0)$. However, in the presence of these two periodic low-frequency forces and with $g = 0$ the solution of the system (2) contains periodic components with certain frequencies other than $2\omega_0$ and $3\omega_0$. However, Q at these frequencies are very weak.

Figure 2 presents $Q(\omega)$ versus g for $\omega = \omega_0$, $4\omega_0$ and $5\omega_0$. In this figure, we find that $Q(\omega_0) \neq 0$ in the absence of a high-frequency force ($g = 0$). However, its value is ≈ 0. When g is varied $Q(\omega)$ at $\omega = \omega_0$, $4\omega_0$, $5\omega_0$ exhibits a resonance. The resonance of $Q(\omega_0)$ is relatively stronger than at the frequencies $4\omega_0$ and $5\omega_0$. We note that the fundamental frequency ω_0 is missing in the input signal $F(t)$. The resonance phenomenon induced by an external noise at a frequency that is absent in the input signal is termed as *ghost-stochastic resonance* [10, 11]. We call the high-frequency

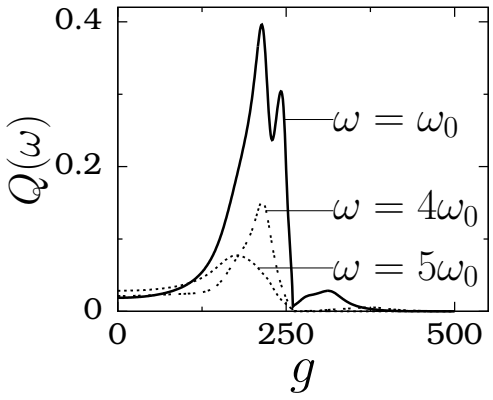

Figure 2: Variation of $Q(\omega)$ with g in the system (2) for the frequencies $\omega = \omega_0$ (= 0.5), $4\omega_0$ and $5\omega_0$ missing in the input signal $F(t)$ (Eq. (1)) with $n = 2$, $k = 2$, $\Delta\omega_0 = 0$ and $f_1 = f_2 = f = 0.1$.

deterministic force induced resonance at the missing frequency of the input signal as *ghost-vibrational resonance*. There are two fundamental differences between the ghost resonance induced by noise and by the high-frequency force. In the noise driven case, when the intensity D of the noise is varied, the signal-to-noise ratio at a missing fundamental frequency becomes maximum at one value of D. Further, the resonances at the frequencies present in the input signal are weak. In the high-frequency induced ghost resonance, the response amplitude can be maximum at more than one value of the parameter g (as shown in Fig. 2). In the system (2), the resonance at the frequencies present in the input signal are stronger than the resonance at the missing fundamental frequency. The resonance at the frequencies $2\omega_0$ and $3\omega_0$ is the well known vibrational resonance.

We numerically compute $g_{\rm VR}$, the value of g at which a first resonance occurs and the corresponding value of the response amplitude, $Q_{\rm max}$, for a range of values of ω_0. The result is shown in Fig. 3. $g_{\rm VR}$ increases almost linearly with ω_0 while $Q_{\rm max}$ decreases nonlinearly with ω_0.

2.2. Theoretical calculation of $Q(\omega_0)$

It is possible to obtain analytical expressions for the response amplitudes $Q(\omega)$ at various values of ω. For the system (2) with $n = 2$ we assume that its solution consists of a low-frequency component X and a high-frequency

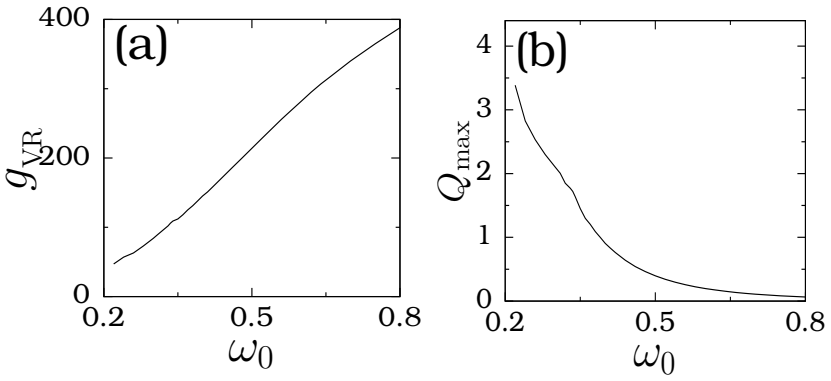

Figure 3: Variation of (a) $g_{\rm VR}$, the value of g at which first resonance at the frequency ω_0 occurs, and (b) $Q_{\rm max}(\omega_0) = Q(g_{\rm VR}, \omega_0)$ with the missing fundamental frequency ω_0 in the input signal in the system (2). The values of the parameters in (1) are as in Fig. 2.

(Ω) component ψ. Substituting $x = X + \psi$ in Eq. (2) we obtain

$$\ddot{X} + d\dot{X} + \alpha X + \beta X^3 + 3\beta X^2\langle\psi\rangle + 3\beta X\langle\psi^2\rangle = f_1\cos\omega_1 t + f_2\cos\omega_2 t, \quad (4)$$

$$\ddot{\psi} + d\dot{\psi} + \alpha\psi + \beta\psi^3 + 3\beta X^2\left(\psi - \langle\psi\rangle\right) + 3\beta X\left(\psi^2 - \langle\psi^2\rangle\right) = g\cos\Omega t, \quad (5)$$

where $\langle\psi^m\rangle = (1/2\pi)\int_0^{2\pi}\psi^m d\tau$ and $\tau = \Omega t$. Since ψ is rapidly oscillating, it is reasonable to approximate the Eq. (5) as $\ddot{\psi} = g\cos\Omega t$, which gives $\psi = -(g/\Omega^2)\cos\Omega t$. For this solution $\langle\psi\rangle = 0$, $\langle\psi^2\rangle = g^2/(2\Omega^4)$ and $\langle\psi^3\rangle = 0$. Then, Eq. (4) becomes

$$\ddot{X} + d\dot{X} + CX + \beta X^3 = f_1\cos\omega_1 t + f_2\cos\omega_2 t, \quad (6)$$

where $C = \alpha + 3\beta g^2/(2\Omega^4)$. Slow oscillations of (6) occur about its stable equilibrium points. Equation (6) with $f_1 = f_2 = 0$ admits three equilibrium points

$$X^* = 0, \ \pm\sqrt{-C/\beta} \ \text{ for } \ g < g_{\rm c} = \left[-\frac{2\alpha\Omega^4}{3\beta}\right]^{1/2} \quad (7)$$

and only one equilibrium point $X^* = 0$ for $g > g_{\rm c}$. For convenience, we introduce the change of variable $Y = X - X^*$. This gives

$$\ddot{Y} + d\dot{Y} + \omega_{\rm r}^2 Y + \beta Y^3 + 3\beta Y^2 X^* = f_1\cos\omega_1 t + f_2\cos\omega_2 t, \quad (8a)$$

where

$$\omega_{\rm r}^2 = \alpha + \frac{3\beta g^2}{2\Omega^4} + 3\beta X^{*2}. \tag{8b}$$

For a weak nonlinearity, an approximate solution of Eq. (8) can be constructed through an iterative process [2], wherein we obtain the sequence of approximations $Y_0(t)$, $Y_1(t)$,$\cdots$ by solving the equations

$$\begin{aligned} \ddot{Y}_0 + d\dot{Y}_0 + \omega_{\rm r}^2 Y_0 &= F(t), & (9)\\ \ddot{Y}_1 + d\dot{Y}_1 + \omega_{\rm r}^2 Y_1 &= F(t) - \beta Y_0^3 - 3\beta X^* Y_0^2 & (10) \end{aligned}$$

and so on. We determine both Y_0 and Y_1. The solution of Eq. (9) in the long time limit is

$$Y_0(t) = A_1 \cos(\omega_1 t + \phi_1) + A_2 \cos(\omega_2 t + \phi_2), \tag{11a}$$

where

$$A_i = \frac{f}{\sqrt{\left(\omega_{\rm r}^2 - \omega_i^2\right)^2 + d^2\omega_i^2}}, \quad \phi_i = \tan^{-1}\left(-\frac{d\omega_i}{\omega_{\rm r}^2 - \omega_i^2}\right), \quad i = 1, 2. \tag{11b}$$

Substituting the above expression for Y_0 in (10), we can find the solution Y_1. In addition to the frequencies ω_1 and ω_2, the solution Y_1 contains certain other frequencies, namely, $l\omega_0$, where $l = 1,\ k-1,\ k,\ k+1,\ k+2,\ 2k,$ $2k+1,\ 2k+2,\ 3k,\ 3k+1,\ 3k+2,\ 3k+3$ due to the terms Y_0^2 and Y_0^3 in Eq. (10). When $k = 2$ the various frequencies present in Y_1 are $\omega = l\omega_0$, $l = 1, 2, \cdots, 9$. The lowest and the highest frequencies in Y_1 are $\omega_2 - \omega_1 = \omega_0$ and $3\omega_2$ respectively.

Retaining only the terms containing ω_0, ω_1, ω_2, $\omega_1 - \omega_0$ (which will become ω_0 if $k = 2$) in the right-side of Eq. (10) we obtain (with $Y_1 = Y_1\ (\omega_0,\ \omega_1,\ \omega_2,\ \omega_1 - \omega_0)$)

$$\begin{aligned} Y_1 &= \frac{a_{01}}{s_0}\cos\left(\omega_0 t + \phi_0 - \phi_1 + \phi_2\right) \\ &\quad + \frac{a_{02}}{s_{01}}\cos\left((\omega_1 - \omega_0)t + \phi_0 + 2\phi_1 - \phi_2\right) \\ &\quad + \frac{a_1}{s_1}\cos\left(\omega_1 t + \phi_1 + \phi_2\right) + \frac{f}{s_1}\cos\left(\omega_1 t + \phi_1\right) \\ &\quad + \frac{a_2}{s_2}\cos\left(\omega_2 t + 2\phi_2\right) + \frac{f}{s_2}\cos\left(\omega_2 t + \phi_2\right), \end{aligned} \tag{12a}$$

where

$$\phi_i = \tan^{-1}\left(-\frac{d\omega_i}{\omega_{\rm r}^2-\omega_i^2}\right), \quad i=0,1,2 \tag{12b}$$

$$\omega_i = (k+i-1)\omega_0+\Delta\omega_0, \quad i=1,2 \tag{12c}$$

$$s_i = \sqrt{\left(\omega_{\rm r}^2-\omega_i^2\right)^2+d^2\omega_i^2}, \quad i=0,1,2 \tag{12d}$$

$$s_{01} = s_0\left(\omega_0\rightarrow\omega_1-\omega_0\right), \quad A_i=\frac{f}{s_i}, \quad i=1,2 \tag{12e}$$

$$a_{01} = 3\beta X^* A_1 A_2, \quad a_{02}=\frac{3}{4}\beta A_1^2 A_2, \tag{12f}$$

$$a_1 = \frac{3}{4}\beta A_1\left(A_1^2+2A_2^2\right), \quad a_2=\frac{3}{4}\beta A_2\left(A_2^2+2A_1^2\right). \tag{12g}$$

For $k=2$ and $\Delta\omega_0=0$ we notice that $\omega_1-\omega_0=\omega_0$. In this case the first two terms in the right-side of Eq. (12a) are periodic with frequency ω_0, otherwise the first term alone is periodic with a frequency ω_0.

In Eq. (12a) for $|f_1=f_2=f|\ll 1$ we can drop the third and fifth terms in the right-side because a_1 and a_2 are of the order of f^3, while the fourth and sixth terms are of the order of f only and the minimum value of s_i is $d\omega_i$ which is not very small for $d=0.5$ and $\omega_0=0.5$. Then the amplitude of the periodic components in the solution (12a) with the frequencies ω_0, ω_1 and ω_2 are

$$A(\omega_1) = \frac{f}{s_1}, \quad A(\omega_2)=\frac{f}{s_2}, \tag{13a}$$

$$A(\omega_0, k=2, \Delta\omega_0=0) = \frac{\sqrt{a_{01}^2+a_{02}^2+2a_{01}a_{02}\cos(2\phi_2-3\phi_1)}}{s_0}, \tag{13b}$$

$$A(\omega_0, k\neq 2 \text{ or } \Delta\omega_0\neq 0) = \frac{a_{01}}{s_0}=\frac{3\beta X^* f^2}{s_0 s_1 s_2}. \tag{13c}$$

Then $Q(\omega_i)=A(\omega_i)/f$.

To verify the theoretical treatment, we plot in Fig. 4 both theoretically and numerically calculated $Q(\omega_0)$, $Q(2\omega_0)$ and $Q(3\omega_0)$ as a function of the parameter g. We notice that theoretical Q at $\omega=\omega_0$, $2\omega_0$ and $3\omega_0$ are in very good agreement with the numerically computed Q.

$Q(\omega_i)$ becomes maximum when $\omega_{\rm r}^2=\omega_i^2$, $i=1,2$. Then, the analytical

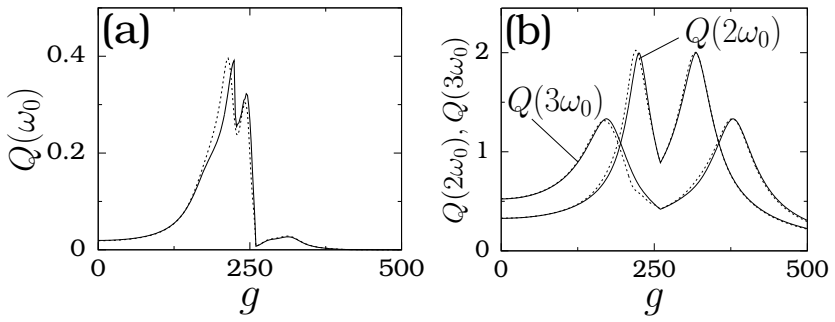

Figure 4: Theoretically calculated (continuous curve) and numerically computed (dashed curve) $Q(\omega_0)$, $Q(2\omega_0)$ and $Q(3\omega_0)$ versus g for the system (2) with $\omega_0 = 0.5$, $n = 2$, $k = 2$, $\Delta\omega_0 = 0$ and $f_1 = f_2 = f = 0.1$.

expressions for g at which resonances occur, denoted as $g_{\rm VR}$, are given by

$$g^{(1)}_{\rm VR}(\omega_i) = \Omega^2 \left[\frac{1}{3\beta}(2|\alpha| - \omega_i^2)\right]^{1/2}, \quad i = 1, 2 \tag{14a}$$

$$g^{(2)}_{\rm VR}(\omega_i) = \Omega^2 \left[\frac{2}{3\beta}(\omega_i^2 + |\alpha|)\right]^{1/2}, \quad i = 1, 2 \tag{14b}$$

where $2|\alpha| > \omega_i^2$. Because $A(\omega_0)$ is a complicated function of g it is very difficult to find an analytical expression for $g_{\rm VR}$ at ω_0.

3. Effect of k, n and $\Delta\omega_0$ on resonance in the single Duffing oscillator

The theoretical procedure employed in the previous section for the determination of an analytical expression for $Q(\omega_0)$ can be extended for $n > 2$. Since such an analysis involves tedious mathematics we perform a numerical simulation. We choose $f_i = f$, $i = 1, 2, \cdots, n$.

Figure 5(a) presents $Q(\omega_0)$ versus g for several values of k with $n = 2$ and $\Delta\omega_0 = 0$. $Q(\omega_0)$ (as well as $Q(\omega_1)$ and $Q(\omega_2)$) decays to zero with k. For $k \neq 2$ the theoretical expression for $A(\omega_0)$ in $Q(\omega_0) = A(\omega_0)/f$ is given by Eq. (13c). For a fixed value of g as k increases the quantities s_i, $i = 0, 1, 2$ increase and A_1 and A_2 decrease. Since $A(\omega_0)$ is directly proportional to A_1, A_2 and $1/s_0$, its value decreases with increasing values of k. We notice in Fig. 5(a) that $Q(\omega_0) = 0$ for $g > g_{\rm c} (= 259.81)$ when $k > 2$. This is because

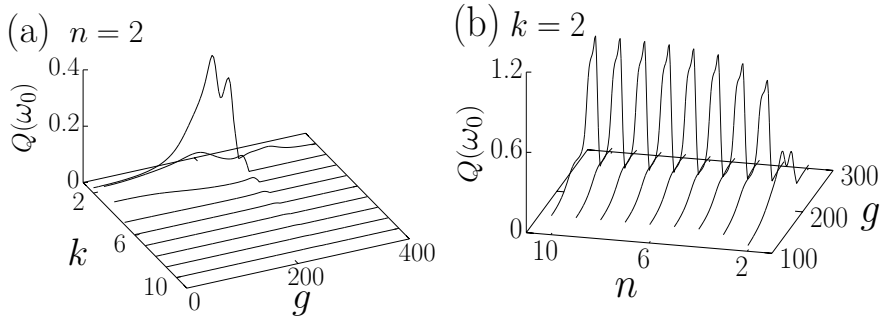

Figure 5: Three-dimensional plot of $Q(\omega_0)$ versus g and (a) k for $n = 2$ and (b) n for $k = 2$ for the system (2) with $\omega_0 = 0.5$ and $f = 0.1$.

for $g > g_c$ the equilibrium point about which a slow oscillation takes place is $X^* = 0$ and hence $Q(\omega_0)$ becomes zero (refer Eq. (13c)). That is, for $k > 2$ the output signal will have a periodic component with the missing frequency ω_0 only if the center of oscillation of the output $x(t)$ is $\neq 0$ which will happen for $g < g_c$. We note that g_c (given by Eq. (7)) depends on the parameters α, β and Ω.

The value of $Q(\omega_0)$ at resonance, as shown in Fig. 5(b), increases with the number of periodic forces, n, and attains a saturation. For $k > 2$ resonance occurs for $n \geq 2$, but the value of $Q(\omega_0)$ at resonance decreases when n increases.

Next, we consider the system (2) with $\Delta\omega_0 \neq 0$. When $\Delta\omega_0 = 0$ the frequencies of the periodic forces in $F(t)$ are integer multiples of the fundamental frequency ω_0. For $\Delta\omega_0 \neq 0$ the frequency difference between successive periodic components remains the same. The frequencies of the periodic components are essentially shifted multiples of ω_0. Each component in $F(t)$ is periodic while the force $F(t)$ is aperiodic, that is, anharmonic. Figure 6(a) displays the effect of $\Delta\omega_0$ on the response the amplitude profile for $k = 2$, $n = 2$ and $\omega_0 = 0.5$. For $\Delta\omega_0 \neq 0$ the amplitude $A(\omega_0)$ given by Eq. (13c) is inversely proportional to $s_0 s_1 s_2$. For a fixed value of g, the quantities s_i, $i = 0, 1, 2$ increase with increase in $\Delta\omega_0$. Consequently, $A(\omega_0)$ and hence $Q(\omega_0) = A(\omega_0)/f$ decrease with increase in $\Delta\omega_0$. This is evident in Fig. 6(a). We observe a similar result in Fig. 6(b) where $Q(\omega_0)$ is plotted as a function of k and g for $n = 2$ and $\Delta\omega_0 = 0.1$. In Fig. 6(c) $Q(\omega_0)$ versus g for various values of n is plotted for $k = 2$ and $\Delta\omega_0 = 0.1$ where $Q(\omega_0)$ attains a saturation. This result is similar to the one shown in Fig. 5(b) for $\Delta\omega_0 = 0$. In all

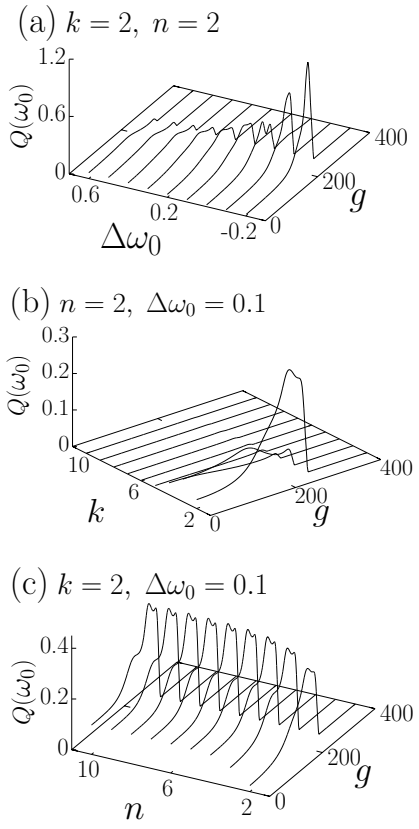

Figure 6: $Q(\omega_0)$ versus g for various values of (a) $\Delta\omega_0$ for $k = 2$, $n = 2$, (b) k for $n = 2$, $\Delta\omega_0 = 0.1$ and (c) n for $k = 2$, $\Delta\omega_0 = 0.1$. In all the cases $\omega_0 = 0.5$ and $f = 0.1$.

the subplots in Fig. 6 $Q(\omega_0) = 0$ for $g > g_{\rm c}(= 259.81)$ because $A(\omega_0) \propto X^*$ and $X^* = 0$ for $g > g_{\rm c}$.

4. Signal propagation in one-way coupled systems

In this section we analyse the features of signal propagation at the missing fundamental frequency in a regular network of one-way coupled $N(= 200)$ units. We consider the cases of multi-frequency signal applied to (i) first unit only and (ii) to all the units.

4.1. Description of the network model

The network essentially consists of N units. The first unit is uncoupled and is alone driven by both a multi-frequency input periodic signal and the high-frequency periodic signal. The interaction is along one direction. We choose the coupling term to be linear and the system representing each unit as the Duffing oscillator. The equation of motion of the network is given by

$$\ddot{x}_1 + d\dot{x}_1 + \alpha x_1 + \beta x_1^3 = F(t) + g\cos\Omega t, \tag{15a}$$

$$\ddot{x}_i + d\dot{x}_i + \alpha x_i + \beta x_i^3 = \delta x_{i-1}, \quad i = 2, 3, \cdots, N \tag{15b}$$

and $F(t)$ is given by Eq. (1). The dynamics of the first oscillator is independent of the dynamics of the other oscillators. We fix the values of the parameters in the network as $d = 0.5$, $\alpha = -2$, $\beta = 1$, $\omega_0 = 0.5$ and $\Omega = 30\omega_0$.

4.2. Undamped signal propagation

In the input signal $F(t)$ the fundamental frequency ω_0 is absent. We numerically calculate the response amplitude $Q_i(\omega_0)$ using Eq. (3). Figure 7(a) shows $Q_i(\omega_0)$ as a function of the unit i for a few fixed values of the coupling strength δ with the values of the parameters in $F(t)$ as $n = 2$, $k = 2$, $\omega_0 = 0.5$, $\Delta\omega_0 = 0$, $f_1 = f_2 = \cdots = f_n = f = 0.1$ and $g = 0$. In the absence of the high-frequency force $Q_1 = 0.01874$. For $\delta < \delta_c = 1.78$, $Q_i < Q_1$ for $i \gg 1$. For $\delta \geq \delta_c$ as i increases the value of Q_i increases slowly then increases rapidly and reaches a saturation. $Q_{200} > Q_1$ and the network displays undamped signal propagation. For very large i the response amplitude Q_i oscillates about a value with small amplitude. Neglecting this small oscillation in Q_i, we notice that Q_i becomes almost constant for sufficiently large values of i. We denote Q_L as the limiting (saturation) value of Q_i. In Fig. 7(a) Q_L increases with increase in δ from δ_c. The undamped and enhanced propagation of signal with the frequency ω_0 missing in the input signal takes place even in the absence of the high-frequency periodic force. The enhanced signal propagation is due to the unidirectional coupling. Note that the input signal $F(t)$ is applied to the first oscillator only.

We plot Q_i versus i for three values of g with $\delta = 2$ in Fig. 7(b). Q_L is independent of the amplitude g. The values of g have a strong influence on Q_i only over a certain range of values of i denoting the oscillators number. In Fig. 7(b) roughly in the 40th to 70th oscillators Q_i varies with g. In this interval of i, Q_i rapidly increases with i. As g increases from 0 the Q_i profile oscillates and becomes stationary for sufficiently large values of g. Similar

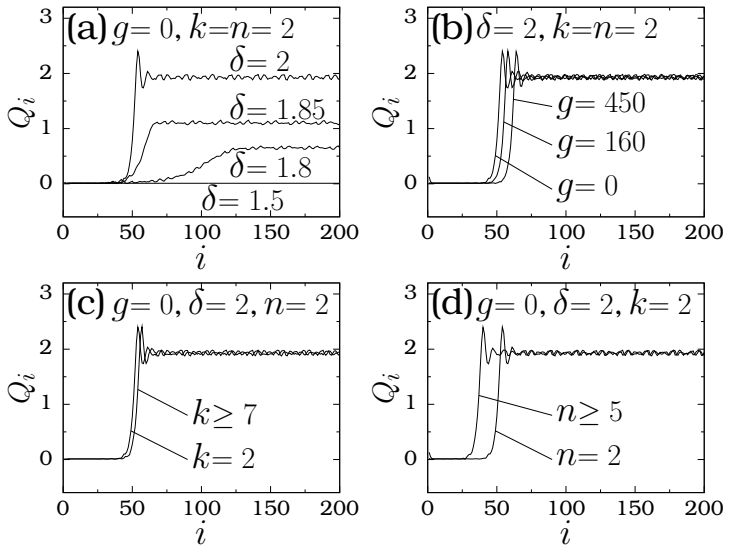

Figure 7: Dependence of Q_i versus i curve on (a) the coupling strength δ for $g = 0$, $k = n = 2$, (b) the amplitude g of the high-frequency periodic force for $\delta = 2$, $k = n = 2$, (c) the parameter k in $F(t)$ for $\delta = 2$, $n = 2$ and $g = 0$ and (d) the number of periodic forces in $F(t)$ for $\delta = 2$, $g = 0$ and $k = 2$. In all the cases $\omega_0 = 0.5$, $f = 0.1$, $\Delta\omega_0 = 0$ and $\Omega = 30\omega_0$. The first oscillator alone is driven by the force $F(t)$ and $g\cos\Omega t$.

effects are found for various fixed values of the parameter k and the number of periodic forces n. Figures 7(c) and (d) report the influence of k and n respectively on Q_i for $\delta = 2$ and $g = 0$. In Fig. 7(c) the Q_i versus i profile evolves to a stationary one with increase in the value of k. The Q_i profile remains the same for $n \geq 5$ in Fig. 7(d). An interesting result is that $Q_{\rm L}$ is independent of g, k and n and depends on δ. A numerical simulation is performed for $\Delta\omega_0 \neq 0$. Results similar to the case $\Delta\omega_0 = 0$ are observed. Furthermore, $Q_{\rm L}$ is found to be independent of $\Delta\omega_0$.

4.3. A network with all the units driven by external forces

Next, we consider the network with all the units driven by the force $F(t)$ and $g\cos\Omega t$ and the units are coupled unidirectionally. The equation of motion of the network is

$$\ddot{x}_1 + d\dot{x}_1 + \alpha x_1 + \beta x_1^3 = F(t) + g\cos\Omega t, \tag{16a}$$

$$\ddot{x}_i + d\dot{x}_i + \alpha x_i + \beta x_i^3 = \delta x_{i-1} + F(t) + g\cos\Omega t, \quad i = 2, 3, \cdots, N \tag{16b}$$

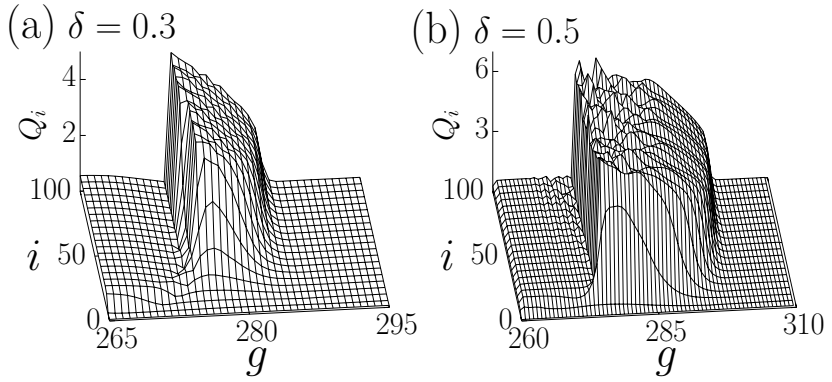

Figure 8: Variation of Q_i with g and i for two values of δ of the network system (16) where $d = 0.5$, $\alpha = -2$, $\beta = 1$, $f = 0.1$, $\omega_0 = 0.5$, $\Omega = 30\omega_0$, $k = 2$, $n = 2$ and $\Delta\omega_0 = 0$.

Figure 8 shows Q_i versus g and i for two fixed values of δ. We observe ghost resonance in each unit. For $\delta = 0.3$ (Fig. 8(a)) the value of Q_i at resonance increases with the unit number i and then reaches a saturation with $Q_{N,\max} > Q_{1,\max}$. For $\delta = 0.5$ (Fig. 8(b)) we can clearly notice small oscillatory variation of Q_i with i for the values of g near resonance. The oscillatory variation of Q_i is found in the network system (15) also. Comparing the Figs. 7 and 8, we observe that the enhancement of the response amplitude at resonance in the network (16) is relatively higher than that of the network (15). Figure 9 presents the variation of $\langle Q \rangle = (1/N) \sum_{i=1}^{N} Q_i(\omega_0)$ with the parameters δ and g.

For the network system (15), in Fig. 7(a) Q of the last unit is < 3 for $\delta < 2$. Furthermore, Q of the last unit is independent of the value of g. For the network system (16), in Fig. 8 Q of the last unit depends on the value of g. Further, in Fig. 9 $\langle Q \rangle$ is > 3 for a wide range of values of δ. In the system (15) undamped signal propagation with $Q_N > Q_1$ occurs for $\delta > 1.78$ and even for $g = 0$. In contrast to this, in the system (16) $Q_N > Q_1$ takes place only for certain range of values of g, however, $\langle Q \rangle > Q_1$ even for a wide range of values of $\delta < 1.78$. As far as the signal amplification and propagation at a missing frequency ω_0 is concerned, driving all units in the unidirectionally coupled system considerably improves the response amplitude over a certain range of values of g and δ compared to the driving the first unit alone.

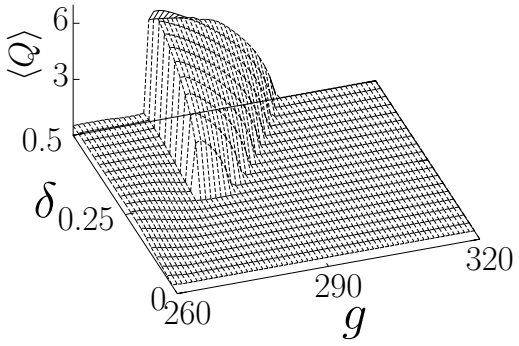

Figure 9: Average response amplitude versus the control parameters δ and g of the network (16) with $f = 0.1$, $\omega_0 = 0.5$, $\Omega = 30\omega_0$, $k = 2$, $n = 2$ and $\Delta\omega_0 = 0$.

5. Conclusion

In a linear system driven by a single periodic force the output contains only the frequency present in the driving force. The response of a nonlinear system to a sinusoidal signal with a single frequency contains the input frequency and its harmonics. When a linear system is subjected to a multi-frequency force, the frequencies present in the output are the same as those in the input. However, changes occur in the magnitudes and phases of the various frequency components. In the case of a nonlinear system driven by a multi-frequency signal, the response not only contains the harmonics of the various input frequencies but inter-modulation components of harmonics can also be generated.

In the present work we have shown the enhancement of response amplitude of a nonlinear system at the missing fundamental frequency in the input multi-frequency signal. In the nonlinear system driven by multi-frequency force and noise, resonance at the missing fundamental frequency is the dominant one and it occurs at a relatively lower value of the noise intensity compared to the resonance at the frequencies present in the input signal. For these types of resonance to occur, the system must have a bistability or excitability. High-frequency induced ghost resonance can occur even in single-well nonlinear systems.

As shown in Fig. 1, the difference between, for example, $Q(2\omega_0)$ when the input signal contains only the frequency $2\omega_0$ and its value when other frequencies are also present in the input signal is negligible. That is, the

response amplitude at a frequency ω present in the input signal is not affected appreciably by the presence of the other frequencies Ω_i, as long as Ω_i are not widely separated from ω. If any of the $\Omega_i \gg \omega$, then the vibrational resonance at the frequency ω occurs.

When the input signal contains only a very few number of periodic components, then it is easy to obtain an analytical expression for the amplitudes of the periodic components with various frequencies. For the single oscillator, $Q(\omega_0)$ decays with the parameters k and $\Delta\omega_0$, while it reaches a saturation with the number of forces. In the network where the oscillators are coupled unidirectionally and only the first oscillator is driven by the external forces, an enhanced and undamped signal propagation at the missing fundamental frequency takes place above a certain critical value of the coupling strength even in the absence of high-frequency force. Moreover, $Q_i(\omega_0)$ becomes constant for sufficiently large values of i. Finally, an interesting result is that, the limiting value of Q is independent of the values of g, k and $\Delta\omega_0$.

Acknowledgment

S. Rajamani expresses her gratitude to University Grants Commission (U.G.C.), Government of India for financial support in the form of U.G.C. meritorious fellowship. MAFS acknowledges financial support from the Spanish Ministry of Science and Innovation under Project No. FIS2009-09898.

References

[1] Lakshmanan M, Rajasekar S. Nonlinear Dynamics: Integrability, Chaos and Patterns. Springer: Berlin; 2003.

[2] Jordan DW, Smith P. Nonlinear Ordinary Differential Equations, Oxford University Press: Oxford; 2007.

[3] Gammaitoni L, Hanggi P, Jung P, Marchesoni F. Stochastic resonance. Rev Mod Phys 1998;70:223-87.

[4] McDonnell MD, Stocks NG, Pearce CEM, Abbott D. Stochastic Resonance. Cambridge University Press: Cambridge; 2008.

[5] Landa PS, McClintok PVE. Vibrational resonance. J Phys A: Math Gen 2000;33:433-38.

[6] Blechman II, Landa PS. Conjugate resonances and bifurcations in nonlinear systems under biharmonical excitation. Int J Nonlin Mech 2004;39:421-26.

[7] Zambrano S, Casado JM, Sanjuan MAF. Chaos-induced resonant effects and its control. Phys Lett A 2007;366:428-32.

[8] Chen YY, Huang PY, Yen JY. Frequency-domain identification algorithms for servo systems with friction. IEEE Transactions on Control Systems Technology. 2002;10:654-65.

[9] Keikha E, Al Mamun A, Lee TH, Bhatia CS. Multi-frequency technique for frequency response measurement and its application to servo system with friction. 18th IFAC World Congress. 2011;5273-78.

[10] Chialvo DR, Calvo O, Gonzalez DL, Piro O, Savino GV. Subharmonic stochastic synchronization and resonance in neuronal systems. Phys Rev E 2002;65:050902(R).

[11] Chialvo DR. How we hear what is not there: A neural mechanism for the missing fundamental illusion. Chaos 2003;13:1226-30.

[12] Buldu JM, Chialvo DR, Mirasso CR, Torrent MC, Garcia-Ojalvo J. Ghost resonance in a semiconductor laser with optical feedback. Europhys Lett 2003;64:178-184.

[13] Buldu JM, Gonzaiez CM, Trull J, Torrent MC, Garcia-Ojalvo J. Coupling-mediated ghost resonance in mutually injected lasers. Chaos 2005;15:013103.

[14] Van der Sande G, Verschaffelt G, Danckaert J, Mirasso CR. Ghost stochastic resonance in vertical-cavity surface-emitting lasers: Experiment and theory. Phys Rev E 2005;72:016113.

[15] Calvo O, Chialvo DR. Ghost stochastic resonance in an electronic circuit. Int J Bifur Chaos 2006;16:731-35.

[16] Lopera A, Buldu JM, Torrent MC, Chialvo DR, Garcia-Ojalvo J. Ghost stochastic resonance with distributed inputs in pulse-coupled electronic neurons. Phys Rev E 2006;73:021101.

[17] Gomes I, Vermellho MVB, Lyra ML. Ghost resonance in the chaotic Chuas circuit. Phys Rev E 2012;85:056201.

[18] Balenzuela P, Garcia-Ojalvo J, Manjarrez E, Martinez L, Mirasso CR. Ghost resonance in a pool of heterogeneous neurons. Biosystems 2007;89:166-72.

[19] El-Bassiouny AF, Abd El-Latif GM. Resonances in nonlinear structure vibrations under multifrequency excitations. Phys Scr 2006;74:410-421.